JAMA Facial Plastic Surgery | Original Investigation

Comparison of Airflow Between Spreader Grafts and Butterfly Grafts Using Computational Flow Dynamics in a Cadaveric Model

Bryan M. Brandon, MD; Grace K. Austin, MD; Gita Fleischman, MD; Saikat Basu, PhD; Julia S. Kimbell, PhD; William W. Shockley, MD; J. Madison Clark, MD

IMPORTANCE Nasal valve compromise is a major cause of nasal obstruction, and multiple methods have been developed to address it.

OBJECTIVE To compare nasal airflow resistance, airflow partitioning, and mucosal cooling (heat flux) before and after 2 surgical interventions, butterfly and spreader graft placement, used to treat nasal valve compromise.

DESIGN, SETTING, AND PARTICIPANTS In this cadaveric tissue study, 4 fresh cadaveric heads underwent both spreader graft and butterfly graft surgical procedures in alternating sequence in March 2016. Preoperative and postoperative computed tomographic scans were used to generate 3-dimensional (3-D) models of the nasal airway. These models were then used in steady state computational fluid dynamics simulations of airflow and heat transfer during inspiration.

INTERVENTION Butterfly and spreader graft techniques.

MAIN OUTCOMES AND MEASURES Nasal airflow resistance, airflow partitioning, and heat flux.

RESULTS Donors 1, 2, and 3 were white males; donor 4, a white female. Computational fluid dynamics simulations during inspiration in 3-D models generated from preoperative and postoperative computed tomographic scans of the 4 cadaveric heads indicated reductions from preoperative values in nasal airflow resistance associated with both butterfly grafts (range, 20%-51%) and spreader grafts (range, 2%-29%). Butterfly grafts were associated with a greater reduction in nasal airflow resistance in models of all 4 cadaveric heads. Changes from preoperative values for heat flux, a biophysical variable that correlates with the subjective sensation of nasal patency, were more variable, ranging from −11% to 4% following butterfly grafts and −9% to 10% following spreader grafts. The preoperative airflow allocation in the left and right nostrils improved consistently with the butterfly graft. With the spreader graft, there were improvements for donors 1 and 4, but the allocations were worse for donors 2 and 3.

CONCLUSIONS AND RELEVANCE The results of this study suggest that the more recently developed butterfly graft technique may be associated with a similar level of improved nasal airflow as that observed with the use of a spreader graft in nasal valve compromise. Both interventions were associated with comparable changes in heat flux. Because this study addressed only static internal nasal valve stenosis, even greater differences in air flow and heat flux between the 2 techniques may be anticipated in a dynamic model. Further investigation in patients is warranted.

LEVEL OF EVIDENCE NA.

JAMA Facial Plast Surg. doi:10.1001/jamafacial.2017.1994
Published online December 14, 2017.

Author Affiliations: Department of Otolaryngology–Head and Neck Surgery, University of North Carolina School of Medicine, Chapel Hill.

Corresponding Author: Bryan M. Brandon, MD, Department of Otolaryngology–Head and Neck Surgery, University of North Carolina School of Medicine, 170 Manning Dr, Chapel Hill, NC 27599 (bryan.brandon@unchealth.unc.edu).

According to the 2010 American Academy of Otolaryngology-Head and Neck Surgery Clinical Consensus Statement, nasal valve compromise (NVC) is "a distinct and primary cause of symptomatic nasal airway obstruction, yet there remain ambiguities and disparities in the diagnosis and management."[1(p48)] Recently, even the use of the term *nasal valve* has been questioned regarding its adequacy in describing the complex 3-dimensional (3-D) gateway through which nasal airflow travels.[2]

The internal nasal valve (INV) is the narrowest part of the nasal airway and is formed by the junction of the upper lateral cartilage, septum, and caudal head of the inferior turbinate. The ideal angle of the INV in white individuals ranges from 10° to 15° and accounts for up to 50% of the nasal resistance in the anatomically normal upper respiratory tract.[3] As described by Poiseuille's law,[4] which states that, with laminar flow, resistance is inversely related to the fourth power of the radius, even small changes in the valve area exponentially change airflow.

The criterion standard surgical technique to correct NVC has been the placement of spreader grafts. Sheen[5] first described this method, which consists of placing 2 cartilage grafts, typically harvested from the septum, between the dorsal attachment of the upper lateral cartilages and the septum. This enables lateral displacement of the upper lateral cartilages and increases the angle of the INV.

The butterfly graft, first introduced by Clark and Cook[6] as an alternative to the spreader graft in secondary rhinoplasty, has gained popularity in addressing NVC in both primary and secondary rhinoplasty.[7-9] This onlay graft fabricated from conchal cartilage is placed over the caudal septum through either a closed or open approach and is sutured to the caudal margins of the upper lateral cartilages.

The reported surgical failure rate of surgery for nasal airway obstruction is as high as 25% to 50%,[10-13] and multiple studies have demonstrated poor correlation between patient-reported symptoms and objective findings.[14-18] New methods of objectively measuring the efficacy of surgical procedures on INV patency are under active investigation. One such method, computational fluid dynamics (CFD), uses anatomically accurate computational models reconstructed from medical imaging data to study nasal airflow, resistance, and other aspects of nasal physiology. Prior studies[19-21] have identified a number of CFD variables that correlate well with patient-reported symptoms. Based on these studies, nasal airflow resistance and heat flux (a measure of mucosal cooling) have emerged as markers of subjective nasal patency.

The goal of this study was to use CFD analysis in cadaveric models to compare 2 surgical procedures designed to address INV compromise. Our primary hypotheses were that (1) CFD-derived nasal resistance is sufficiently sensitive to distinguish anatomical changes in the INV after spreader and butterfly graft placements and (2) the butterfly graft is associated with reduced nasal airflow resistance, and thus improved nasal airflow, comparable to that associated with a spreader graft. A secondary hypothesis was that the mean heat flux change over main nasal cavity walls is insignificant when surgical alterations are confined to the INV.

Key Points

Question Are butterfly and spreader grafts associated with reduced nasal airflow resistance following surgical intervention for nasal valve compromise?

Findings Computational fluid dynamics analysis conducted in models derived from 4 cadaveric heads indicated a reduction in nasal airflow resistance from preoperative values after placement of either a butterfly graft (range, 20%-51%) or a spreader graft (range, 2%-29%). The butterfly graft was associated with greater reduction in nasal airflow resistance in all 4 cadaveric specimens.

Meaning Spreader and butterfly grafts are associated with comparable reductions in nasal airflow resistance in a cadaveric computational fluid dynamics model.

Figure 1. Study Plan

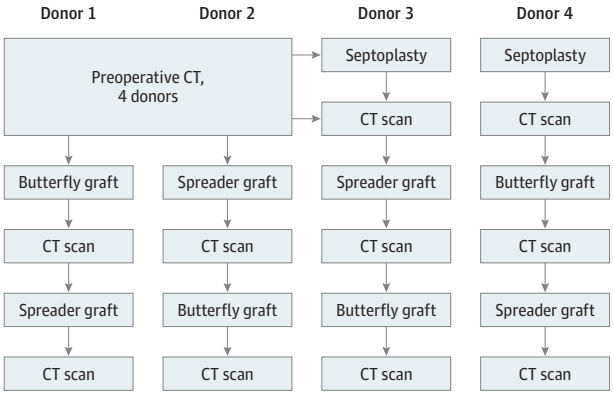

Each cadaveric head underwent a preoperative computed tomographic (CT) scan followed by the treatment plan depicted. Two of the donor specimens required septoplasty prior to either spreader (donor 3) or butterfly (donor 4) graft placement.

Methods

The institutional review board at the University of North Carolina School of Medicine, Chapel Hill, determined that because this study used only human cadaveric tissue it was exempt from their review.

Specimens and Surgical Procedures

Cadaveric Dissections

Four fresh cadaveric heads were obtained (Life Science Anatomical) and nasal cavities cleansed. Each of the 4 cadaveric heads underwent external examination, anterior rhinoscopy using nasal speculum and nasal endoscopy, and cone beam computed tomographic (CT) scan (3D Accuitomo 170; Morita) prior to surgical intervention. Each cadaveric specimen underwent a treatment plan (**Figure 1**) to determine changes in the measured values associated with the specific graft procedure, alternating the order in which the spreader or butterfly graft was placed to avoid bias inherent in conducting all procedures in the same sequence.

Septoplasty

The results of anterior rhinoscopy indicated that 2 of the 4 cadaveric heads had significant septal deviation. Septoplasty was performed on the 2 cadaveric heads with septal deviations before baseline CT scans were obtained for 2 reasons: graft material was needed for the spreader grafts, and a severely deviated nasal septum might introduce a confounding variable when assessing airflow through the nasal passageway. The septoplasty was performed using a hemitransfixion incision in the standard fashion, and the grafts were placed in saline for later use.

Spreader Graft Placement

A standard external rhinoplasty approach was used via transcolumellar and marginal incisions. The soft-tissue envelope was elevated in a subnasal superficial muscular aponeurotic system plane to the rhinion and a subperiosteal plane to the nasion. The upper lateral cartilages were sharply released from the dorsal septum. Spreader grafts were carved from previously harvested septal cartilage measuring 1.7 × 0.4 cm each. The same spreader grafts were used for each cadaveric head. The spreader grafts were placed bilaterally and sutured between the septum and upper lateral cartilages using 5-0 polydioxanone horizontal mattress sutures. The incisions were closed with 5-0 chromic and 6-0 polypropylene sutures in the marginal and transcolumellar incisions, respectively.

Butterfly Graft Placement

A 3-cm curvilinear incision was made in the antihelical fold, and an anteriorly based flap was developed in a subperichondrial plane primarily in the concha cavum portion of the conchal bowl. A 2.5 × 1.5-cm cartilage graft was harvested, preserving the posterior perichondrium. An intercartilaginous incision was then made and a subnasal superficial muscular aponeurotic system plane was developed cephalad to the rhinion. The harvested conchal cartilage was carved into the standard shape, with a final dimension of 2 × 1 cm. The caudal margin of the graft was sutured to the caudal margin of the upper lateral cartilage at 2 points on each side using 5-0 polydioxanone sutures. The intercartilaginous incisions were closed with 5-0 chromic sutures.

After each intervention, the soft-tissue envelope was redraped and incisions were closed. Computed tomographic scans (0.33-mm pixels, 0.66-mm increments) of the entire nasal cavity and external nasal soft tissue were obtained.

Modeling and Simulations

Nasal Model Construction

Computed tomographic scans were imported to medical imaging software (Mimics, version 18.0; Materialise, Inc) to generate realistic 3-D reconstructions. On the basis of visual inspection, a threshold of 300 Hounsfield units was used to delineate the imaged nasal airspace. To ensure anatomical accuracy, thresholding was followed by selective hand editing of the identified pixel domains. In addition, the paranasal sinuses were removed (**Figure 2**A) to reduce model complexity and facilitate heat flux estimation along the main nasal cavity walls.

The following 3 hybrid models were developed for each cadaveric head to determine changes in the measured values associated with the specific surgical intervention as well as to minimize tissue decay artifacts and anatomical variations in the airway distal to the INV: (1) a preoperative nasal airway model that incorporated septoplasty performed on 2 of the cadaveric heads; (2) an airway model with the butterfly graft; and (3) an airway model with the spreader graft. This was implemented by coregistering and smoothly blending an anterior segment of the nasal airway containing the INV, which was defined as 5 mm cephalad from the rhinion to the nostrils, from each of the interventions with the corresponding posterior portion of the preoperative model (Figure 2B). This resulted in a total of 12 separate 3-D models for CFD analysis.

CFD Simulations

The hybrid 3-D models were exported from the medical imaging software in stereolithography file format to computer-aided design and meshing software (ICEM CFD, version 15.0; ANSYS, Inc). A 2-cm-long outlet tube was added to the nasopharynx to ensure fully developed outlet flow in the CFD simulations. Left and right nostril inlets were created using planar cuts at nostril rims. The models were then meshed using approximately 4 million unstructured, graded, tetrahedral elements (Figure 2C).[22,23] Mesh quality was checked for distortion by confirming that all the cells had an aspect ratio exceeding 0.3, as recommended in the ANSYS ICEM CFD manual.

Airflow and heat transport simulations were performed with CFD software (Fluent, version 14.5; ANSYS, Inc.), which uses a finite volume approach at a resting flow rate (15 L/min) under steady state, pressure-driven, laminar conditions.[20,24,25] Although nasal airflow may sometimes devolve into turbulence, at resting breathing it has been shown to maintain a laminar flow profile.[26,27] The simulations used the following boundary conditions: (1) no slip ("zero velocity") at airway walls (simulating the surrounding tissue surfaces) and (2) an inlet pressure set to atmospheric pressure and an inlet to outlet negative pressure gradient that produced a steady inspiratory flow (15 L/min) (Figure 2C). The referenced characteristic values included the following: air density, 1.204 kg/m^3; dynamic viscosity of air, 1.825×10^{-5} kg/(m · s); thermal conductivity of air, 0.0268 W/(m · K); and specific heat of air, 1005.9 J/(kg · K).[19] The air temperature at the nostril inlets was set at 20°C, and the mucosal temperature at the tissue walls was set at 32.6°C.[25,28]

Postprocessing

The CFD software was used to estimate unilateral and bilateral transnasal pressure drop in pascals from nostrils to choanae (posterior end of the septum), unilateral and bilateral volumetric airflows in milliliters per second, and unilateral heat flux in watts per square meter. Nasal resistance and airflow partitioning were calculated as follows:

$$\text{Nasal Resistance} = \Delta P/Q,$$

where ΔP is the transnasal pressure drop from the nostrils to the choanae in pascals, and Q is the volumetric flow rate in milliliters per second; and

$$\text{Airflow Partitioning} = 100\% \times [(\text{Unilateral Flow Rate})/(\text{Total Flow Rate})].$$

Postprocessing visualization was conducted using the CFD software package.

Figure 2. Three-Dimensional Model Generation From Computed Tomographic Scans and Subsequent Meshing

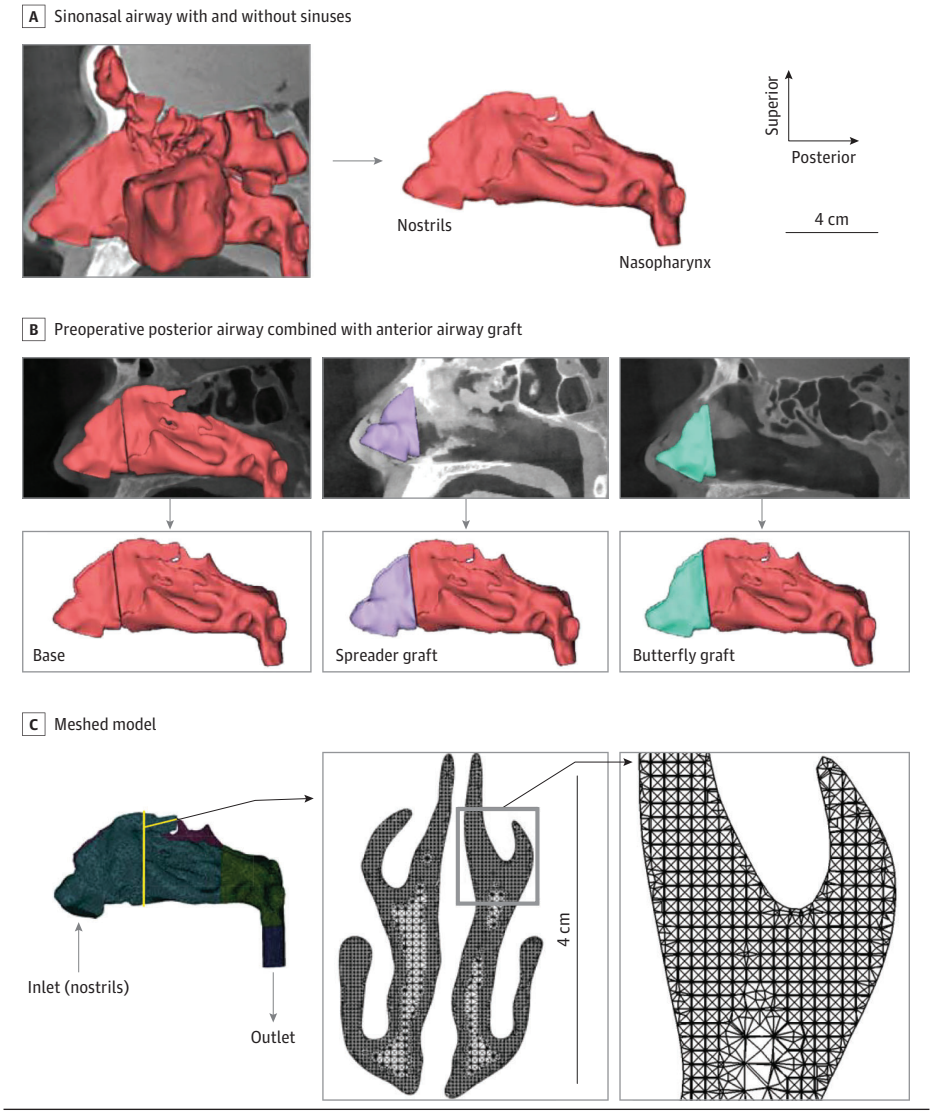

A, Representative 3-dimensional models of the sinonasal airway before (left) and after (right) the sinuses were digitally removed. B, Reconstructions showing the anterior airway following spreader or butterfly graft placement combined with the preoperative posterior airway. C, Inlet and outlet of the computational meshed model. Insets show a coronal cross section of the model mesh.

Results

Nasal Airflow Resistance

Donors 1, 2, and 3 were white males and donor 4 was a white female. Nasal airflow resistance was reduced by both interventions in all 4 cadaveric heads, but the butterfly graft was associated with a greater reduction in nasal airflow resistance in all cases. Reductions in nasal airflow resistance from preoperative values for the butterfly graft ranged from 20% to 51%, whereas that for the spreader grafts ranged from 2% to 29% (**Figure 3**A). Pressure on the main nasal cavity walls was also reduced from the preoperative model in all graft models, but the reduction was more pronounced in the butterfly model than in the spreader model in all 4 donors (Figure 3B).

Airflow Partitioning

Airflow partitioning or airflow allocation is defined as the percentage of airflow that passes through either the left or the right nasal passage. Improvement in airflow partitioning is defined as a more even distribution of airflow (close to 50% for each nasal passage) after surgery. In all cases, the butterfly graft either improved or did not appreciably change the airflow allocation. In donor 1, the spreader graft outperformed the butterfly graft, resulting in an even distribution (50% each) between the 2 sides. However, in donors 2 and 3, airflow allocation was more divergent following placement of the spreader graft than that with the butterfly graft. In donor 4, airflow distribution was improved with both butterfly and spreader grafts, with the butterfly graft more closely approximating an even distribution (**Figure 4**).

Heat Flux

Heat flux is a biophysical CFD variable that correlates with the subjective sensation of nasal patency.[19,21,29] Changes from preoperative values for heat flux after butterfly graft placement ranged from −11% to 4%; for the spreader graft, −9% to 10% (**Figure 5**).

Figure 3. Variation of Nasal Resistance and Representative Wall Pressure Plots

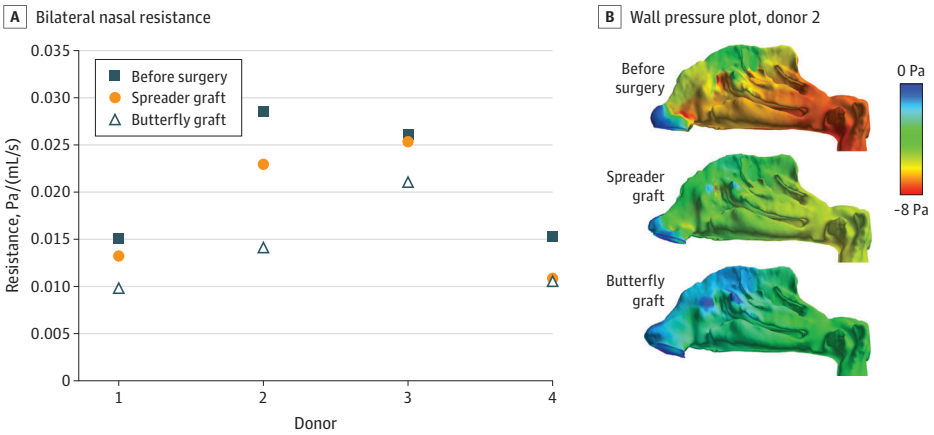

A, Nasal resistance from nostrils to choanae for each model derived from each donor. B, Left lateral view of wall pressure contours plotted on the main nasal cavity walls of donor 2. Blue indicates atmospheric pressure; red, negative pressure.

Secondary Results

The results were not changed by the order of surgical intervention. The same trend for nasal resistance was observed in each of the 4 cadaveric heads, with each case demonstrating the highest resistance preoperatively, the most substantial reduction in resistance with the butterfly graft, and an intermediate reduction in resistance with the spreader graft. This result was observed not only for the sequence of the procedures but also for the presence or absence of prior septoplasty.

Discussion

Nasal valve compromise is now recognized as a distinct entity that can contribute to symptomatic nasal airway obstruction.[1,5,30,31] However, many conditions can mimic or coexist with NVC, making it difficult to treat. In addition, patients may have multilevel obstruction. Thus, it is important to use objective measures to help identify optimal interventions in addressing NVC and improving nasal airflow.[32] In doing so, it may be possible to improve surgical outcomes by using virtual modeling preoperatively to determine surgical interventions that are most effective at managing patient symptoms.

The butterfly graft is currently acknowledged as a powerful technique for repairing the INV, but the spreader graft remains the criterion standard. Analysis using CFD has emerged as a useful tool to provide objective data on nasal physiology, and several studies have used CFD to analyze the effects of septoplasty, inferior turbinate reduction, spreader grafts, and other interventions aimed at addressing problems associated with the INV.[33-37] However, to our knowledge no CFD study has yet directly compared the use of spreader and butterfly grafts alone.

The present study expands on the results of a previously described fresh cadaveric model using CFD to directly compare 2 surgical techniques in repair of NVC.[36] The present preliminary results offer objective evidence that CFD-derived nasal resistance may be sufficiently sensitive to detect anatomical changes in the INV after placement of spreader and butterfly grafts. Although the results indicated that butterfly grafts reduced nasal resistance comparable to spreader grafts, the results also suggested that mucosal cooling changes associated with these grafts was relatively small. Several studies have suggested that changes in nasal mucosal cooling are correlated more with changes in subjective sensation of nasal patency than with changes in nasal airflow resistance.[17,19,25] However, these comparisons were made in healthy individuals or patients undergoing surgical procedures involving the main nasal cavity. Further research is needed to study CFD-derived nasal resistance and heat flux and their correlations to symptom abatement in patients undergoing surgical procedures of the INV alone.

The results of this study contribute to a growing body of evidence that suggests that the butterfly graft may be at least as effective as the spreader graft in improving nasal airflow in NVC.[8,9,38] Moreover, several recent studies[39-41] have questioned the efficacy of the spreader graft as the sole intervention aimed at improving nasal airflow through the INV. In one such study, Park[40] found an improvement in the INV angle only when combining a flaring suture with spreader grafts.

Abnormalities in the 4 components of the INV produce varying levels of compromise to airflow resistance, airflow partitioning, and heat flux. Compromise typically is associated proportionally with the cross-sectional area of the INV. According to Poiseuille's law, airflow resistance is inversely proportional to the fourth power of the nasal valve radius. Thus, very small increases in nasal valve radius produce exponential reductions in airflow resistance. It is generally accepted that both the butterfly graft and the spreader graft decrease resistance by increasing the cross-sectional area at the apex of the INV.

However, other physics principles can also be applied to understand airflow through the INV. According to the Bernoulli principle, fluids with increasing velocities experience an associated decrease in pressure in narrowed segments of a collapsible tube. Thus, as airflow increases through the narrowed nasal valve, there is an associated drop in transluminal pressure, resulting in dynamic collapse of the nasal sidewall. At a critical point during inspiration, consistent with the combination of Poiseuille's law, the Bernoulli principle, and the structural integrity of the soft tissues comprising the na-

Figure 4. Airflow Allocation in Left and Right Nasal Passages as a Percentage of Total Nasal Airflow

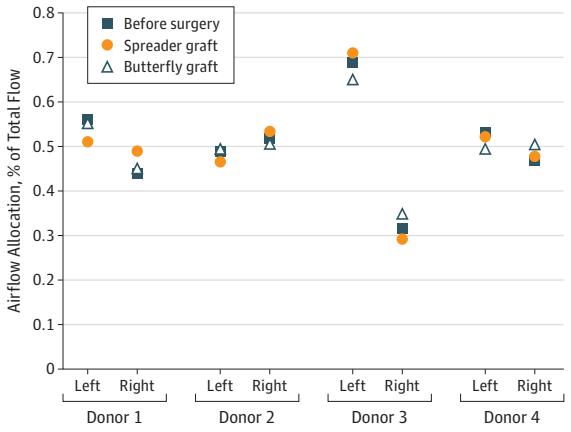

Figure 5. Heat Flux Measured Along the Main Nasal Airway From the Nostrils to the Choanae

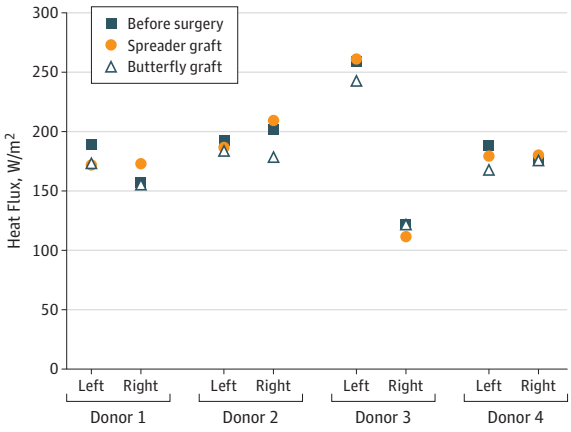

sal valve, increased force of inspiration ceases to increase nasal airflow. Although such idealizations may ignore effects such as wall stress and circulatory flows and assume a streamlined geometry,[2] they may still provide information on the features fundamental to airflow.

We believe that the butterfly graft differs from the spreader graft primarily through lateral wall support and the Bernoulli principle. Through use of the dorsal septum as a fulcrum and secured to the caudal margins of the upper lateral cartilage, the butterfly graft helps provide rigidity to the lateral nasal wall to resist dynamic collapse of the valve with inspiration. By contrast, use of a spreader graft improves nasal resistance through an increase in the radius (Poiseuille's law) but has no effect on the structural integrity of a weakened nasal sidewall to counteract collapse (consistent with the Bernoulli principle). Thus, because this study addresses only static INV collapse, we would anticipate even greater differences in the outcomes between the 2 techniques using a dynamic model.

Careful preoperative cosmetic analysis should be performed when addressing NVC to evaluate whether a patient's nose can accommodate a butterfly graft. Nasal aesthetics that may make a butterfly graft less desirable include very thin skin or a narrow bony nasal dorsum. In such patients, it may be more difficult to camouflage the butterfly graft while maintaining favorable dorsal aesthetic lines.[42] Dissatisfaction regarding the cosmetic outcome from butterfly graft placement has been reported to range from 3% to 19% in several case series.[6-9] Consequently, recent modifications to the butterfly graft have been made to mitigate the risk of a negative cosmetic outcome.[38] It is hoped that studies such as the present one as well as modifications enabling better cosmetic outcomes will help expand the indications for butterfly graft use in repairing NVC.

Limitations

Limitations of this study include the small cohort size from the limited number of donors, which prevented the use of statistical analyses. Cadaveric tissue, although obtained fresh, lacks the resiliency of living tissues. Septoplasty, necessary to obtain graft material, was performed on 2 of the cadaveric heads. To minimize this as a confounding variable, septoplasty was performed prior to the primary data collection. In addition, every effort was made to efficiently and expeditiously perform all surgical procedures to minimize the effect of tissue degradation, and our use of cadaveric models prevented nasal cycling from being a confounding factor in our analyses. However, our simulations did not account for dynamic changes in tissue, such as the collapse of the INV with inspiration.

Conclusions

The goal of this study was to validate a methodology and identify CFD variables that are sufficiently sensitive to measure differences between surgical techniques targeting the INV. Our preliminary CFD data suggested that in a static cadaveric model, the butterfly graft compares favorably to the spreader graft in nasal resistance, airflow partitioning, and heat flux. These findings support continuing this research in clinical trials to compare results from different surgical techniques to address NVC.

ARTICLE INFORMATION

Accepted for Publication: October 1, 2017.

Published Online: December 14, 2017. doi:10.1001/jamafacial.2017.1994

Author Contributions: Dr Brandon had full access to all the data in the study and takes responsibility for the integrity of the data and the accuracy of the data analysis.

Study concept and design: All authors.
Acquisition, analysis, or interpretation of data: Brandon, Austin, Fleischman, Basu, Kimbell, Clark.
Drafting of the manuscript: Brandon, Fleischman, Basu, Clark.
Critical revision of the manuscript for important intellectual content: Brandon, Austin, Basu, Kimbell, Shockley, Clark.
Statistical analysis: Basu.
Obtained funding: Austin, Kimbell.
Administrative, technical, or material support: All authors.
Study supervision: Austin, Kimbell, Shockley, Clark.

Conflict of Interest Disclosures: None reported.

Funding/Support: Dr Austin is supported by a grant (T32DC005360) from the National Institute of Deafness and other Communicative Disorders. Dr Basu is supported by a grant (R01 HL122154)

from the National Heart, Lung, and Blood Institute. Funds from the Department of Otolaryngology–Head and Neck Surgery, University of North Carolina School of Medicine, were used to procure the cadaveric heads and to conduct the CT scans.

Role of the Funder/Sponsor: The funders had no role in the design and conduct of the study; collection, management, analysis, and interpretation of the data; preparation, review, or approval of the manuscript; and decision to submit the manuscript for publication.

Disclaimer: The contents of this article are solely the responsibility of the authors and do not necessarily represent the official views of the National Institutes of Health.

Additional Contributions: Carla Sibrian of University of North Carolina Healthcare provided technical assistance during the computed tomographic scanning. She was not compensated by our group for this contribution.

REFERENCES

1. Rhee JS, Weaver EM, Park SS, et al. Clinical consensus statement: diagnosis and management of nasal valve compromise. *Otolaryngol Head Neck Surg*. 2010;143(1):48-59.

2. Tripathi PB, Elghobashi S, Wong BJF. The myth of the internal nasal valve. *JAMA Facial Plast Surg*. 2017;19(4):253-254.

3. Schlosser RJ, Park SS. Functional nasal surgery. *Otolaryngol Clin North Am*. 1999;32(1):37-51.

4. Sutera SP, Skalak R. The history of Poiseuille's law. *Annu Rev Fluid Mech*. 1993; 25(1):1-20.

5. Sheen JH. Spreader graft: a method of reconstructing the roof of the middle nasal vault following rhinoplasty. *Plast Reconstr Surg*. 1984;73 (2):230-239.

6. Clark JM, Cook TA. The "butterfly" graft in functional secondary rhinoplasty. *Laryngoscope*. 2002;112(11):1917-1925.

7. Akcam T, Friedman O, Cook TA. The effect on snoring of structural nasal valve dilatation with a butterfly graft. *Arch Otolaryngol Head Neck Surg*. 2004;130(11):1313-1318.

8. Friedman O, Cook TA. Conchal cartilage butterfly graft in primary functional rhinoplasty. *Laryngoscope*. 2009;119(2):255-262.

9. Stacey DH, Cook TA, Marcus BC. Correction of internal nasal valve stenosis: a single surgeon comparison of butterfly versus traditional spreader grafts. *Ann Plast Surg*. 2009;63(3):280-284.

10. Singh A, Patel N, Kenyon G, Donaldson G. Is there objective evidence that septal surgery improves nasal airflow? *J Laryngol Otol*. 2006;120 (11):916-920.

11. André RF, D'Souza AR, Kunst HP, Vuyk HD. Sub-alar batten grafts as treatment for nasal valve incompetence. *Rhinology*. 2006;44(2):118-122.

12. Dinis PB, Haider H. Septoplasty: long-term evaluation of results. *Am J Otolaryngol*. 2002;23(2): 85-90.

13. Illum P. Septoplasty and compensatory inferior turbinate hypertrophy: long-term results after randomized turbinoplasty. *Eur Arch Otorhinolaryngol*. 1997;254(suppl 1):S89-S92.

14. Kjærgaard T, Cvancarova M, Steinsvåg SK. Does nasal obstruction mean that the nose is obstructed? *Laryngoscope*. 2008;118(8):1476-1481.

15. Lam DJ, James KT, Weaver EM. Comparison of anatomic, physiological, and subjective measures of the nasal airway. *Am J Rhinol*. 2006;20(5):463-470.

16. Pawar SS, Garcia GJ, Kimbell JS, Rhee JS. Objective measures in aesthetic and functional nasal surgery: perspectives on nasal form and function. *Facial Plast Surg*. 2010;26(4):320-327.

17. Rhee JS. Measuring outcomes in nasal surgery: realities and possibilities. *Arch Facial Plast Surg*. 2009;11(6):416-419.

18. Schumacher MJ. Nasal congestion and airway obstruction: the validity of available objective and subjective measures. *Curr Allergy Asthma Rep*. 2002;2(3):245-251.

19. Kimbell JS, Frank DO, Laud P, Garcia GJ, Rhee JS. Changes in nasal airflow and heat transfer correlate with symptom improvement after surgery for nasal obstruction. *J Biomech*. 2013;46(15): 2634-2643.

20. Kimbell JS, Garcia GJ, Frank DO, Cannon DE, Pawar SS, Rhee JS. Computed nasal resistance compared with patient-reported symptoms in surgically treated nasal airway passages. *Am J Rhinol Allergy*. 2012;26(3):e94-e98.

21. Sullivan CD, Garcia GJ, Frank-Ito DO, Kimbell JS, Rhee JS. Perception of better nasal patency correlates with increased mucosal cooling after surgery for nasal obstruction. *Otolaryngol Head Neck Surg*. 2014;150(1):139-147.

22. Basu S, Witten N, Kimbell J. Influence of localized mesh refinement on numerical simulations of post-surgical sinonasal airflow [abstract 252]. *J Aerosol Med Pulm Drug Deliv*. 2017; 30(3):A-14.

23. Frank-Ito DO, Wofford M, Schroeter JD, Kimbell JS. Influence of mesh density on airflow and particle deposition in sinonasal airway modeling. *J Aerosol Med Pulm Drug Deliv*. 2015;29(1):46-56.

24. Basu S, Kimbell JS, Zanation AM, Ebert CS, Senior BA. Clinical questions and the role CFD can play. Presented at the 69th American Physical Society, Division of Fluid Dynamics, Annual Meeting; November 21, 2016; Portland, Oregon.

25. Garcia GJ, Bailie N, Martins DA, Kimbell JS. Atrophic rhinitis: a CFD study of air conditioning in the nasal cavity. *J Appl Physiol (1985)*. 2007;103(3): 1082-1092.

26. Garlapati RR, Lee HP, Chong FH, Wang Y. Indicators for the correct usage of intranasal medications: a computational fluid dynamics study. *Laryngoscope*. 2009;119(10):1975-1982.

27. Shanley KT, Zamankhan P, Ahmadi G, Hopke PK, Cheng Y-S. Numerical simulations investigating the regional and overall deposition efficiency of the human nasal cavity. *Inhal Toxicol*. 2008;20(12): 1093-1100.

28. Lindemann J, Leiacker R, Rettinger G, Keck T. Nasal mucosal temperature during respiration. *Clin Otolaryngol Allied Sci*. 2002;27(3):135-139.

29. Zhao K, Blacker K, Luo Y, Bryant B, Jiang J. Perceiving nasal patency through mucosal cooling rather than air temperature or nasal resistance. *PLoS One*. 2011;6(10):e24618.

30. Constantian MB. The incompetent external nasal valve: pathophysiology and treatment in primary and secondary rhinoplasty. *Plast Reconstr Surg*. 1994;93(5):919-931.

31. Constantian MB, Clardy RB. The relative importance of septal and nasal valvular surgery in correcting airway obstruction in primary and secondary rhinoplasty. *Plast Reconstr Surg*. 1996;98 (1):38-54.

32. Ballert JA, Park SS. Functional rhinoplasty: treatment of the dysfunctional nasal sidewall. *Facial Plast Surg*. 2006;22(1):49-54.

33. Chen XB, Leong SC, Lee HP, Chong VF, Wang DY. Aerodynamic effects of inferior turbinate surgery on nasal airflow—a computational fluid dynamics model. *Rhinology*. 2010;48(4):394-400.

34. Chen XB, Lee HP, Chong VF, Wang DY. Assessment of septal deviation effects on nasal air flow: a computational fluid dynamics model. *Laryngoscope*. 2009;119(9):1730-1736.

35. Garcia GJ, Rhee JS, Senior BA, Kimbell JS. Septal deviation and nasal resistance: an investigation using virtual surgery and computational fluid dynamics. *Am J Rhinol Allergy*. 2010;24(1):e46-e53.

36. Shadfar S, Shockley WW, Fleischman GM, et al. Characterization of postoperative changes in nasal airflow using a cadaveric computational fluid dynamics model: supporting the internal nasal valve. *JAMA Facial Plast Surg*. 2014;16(5):319-327.

37. Wexler D, Segal R, Kimbell J. Aerodynamic effects of inferior turbinate reduction: computational fluid dynamics simulation. *Arch Otolaryngol Head Neck Surg*. 2005;131(12):1102-1107.

38. Loyo M, Gerecci D, Mace JC, Barnes M, Liao S, Wang TD. Modifications to the butterfly graft used to treat nasal obstruction and assessment of visibility. *JAMA Facial Plast Surg*. 2016;18(6):436-440.

39. Schlosser RJ, Park SS. Surgery for the dysfunctional nasal valve: cadaveric analysis and clinical outcomes. *Arch Facial Plast Surg*. 1999;1(2): 105-110.

40. Park SS. The flaring suture to augment the repair of the dysfunctional nasal valve. *Plast Reconstr Surg*. 1998;101(4):1120-1122.

41. Rohrich RJ, Pulikkottil BJ, Stark RY, Amirlak B, Pezeshk RA. The importance of the upper lateral cartilage in rhinoplasty. *Plast Reconstr Surg*. 2016; 137(2):476-483.

42. Chaiet SR, Marcus BC. Nasal tip volume analysis after butterfly graft. *Ann Plast Surg*. 2014;72(1):9-12.